Manipulating Atoms with Photons

Claude Cohen-Tannoudji and Jean Dalibard,
Laboratoire Kastler Brossel* and Collège de France,
24 rue Lhomond, 75005 Paris, France

*Unité de Recherche de l'Ecole normale supérieure et de l'Université Pierre et Marie Curie, associée au CNRS.

Contents

1 Introduction

Electromagnetic interactions play a central role in low energy physics, chemistry and biology. They are responsible for the cohesion of atoms and molecules and are at the origin of the emission and absorption of light by such systems. They can be described in terms of absorptions and emissions of *photons* by charged particles or by systems of charged particles like atoms and molecules. Photons are the energy quanta associated with a light beam. Since the discoveries of Planck and Einstein at the beginning of the last century, we know that a plane light wave with frequency ν, propagating along a direction defined by the unit vector $\boldsymbol{u}$, can be also considered as a beam of photons with energy $E = h\nu$ and linear momentum $\boldsymbol{p} = (h\nu/c)\,\boldsymbol{u}$. We shall see later on that these photons also have an angular momentum along $\boldsymbol{u}$ depending on the polarization of the associated light wave.

Conservation laws are very useful for understanding the consequences of atom-photon interactions. They express that the total energy, the total linear momentum, the total angular momentum are conserved when the atom emits or absorbs a photon. Consider for example the conservation of the total energy. Quantum mechanics tells us that the energy of an atom cannot take any value. It is quantized, the possible values of the energy forming a discrete set E_a, E_b, E_c, ...In an emission process, the atom goes from an upper energy level E_b to a lower one E_a and emits a photon with energy $h\nu$. Conservation of the total energy requires

$$E_b - E_a = h\nu \tag{1}$$

The energy lost by the atom going from E_b to E_a is carried away by the photon.

According to Equation (1), the only possible frequencies emitted by an atom are those corresponding to the energy differences between pairs of energy levels of this atom. This important result means that light is an essential source of information on the atomic world. By measuring the frequencies emitted or absorbed by an atom, it is possible to determine the differences $E_b - E_a$ and thus to obtain the energy diagram of this atom. This is what is called *spectroscopy*. High resolution spectroscopy provides very useful information on the internal dynamics of the atom. Furthermore, each atom has its own spectrum. The frequencies emitted by a hydrogen atom are different from those emitted by a sodium or a rubidium atom. The spectrum of frequencies emitted by an atom is in some way its finger prints. It is thus possible to collect information on the constituents of different types of media by observing the light originating from these media.

During the last few decades, it has been realized that light is not only a source of information on atoms, but also a tool which can be used to act on them, to manipulate them, to control their various degrees of freedom. These methods are also based on conservation laws and use the transfer of angular and linear momentum from photons to atoms. With the development of laser sources, this research field has considerably expanded during the last few years. Methods have been developed to polarize atoms, to trap them and to cool them to very low temperatures. New perspectives have been opened

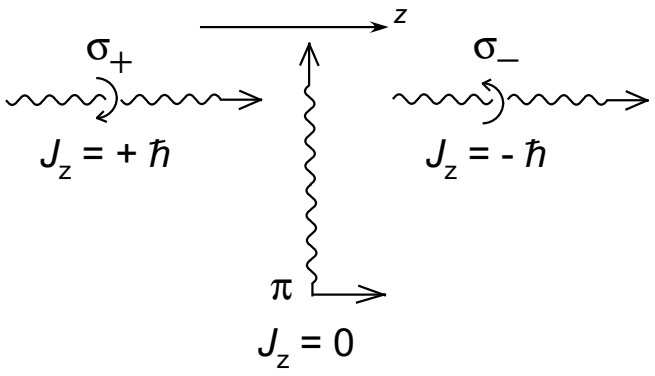

FIGURE 1: Three different states of polarization of a photon and corresponding values of J_z

in various domains like atom clocks, atomic interferometry, Bose-Einstein condensation. The purpose of this article is to review the physical processes which are at the basis of this research field, and to present some of its most remarkable applications. Other applications are also described in two other articles of this book.

Two types of degrees of freedom have to be considered for an atom: (i) the internal degrees of freedom, such as the electronic configuration or the spin polarization, in the center of mass reference frame; (ii) the external degrees of freedom, *i.e.* the position and the momentum of the center of mass. In section 2 we present the basic concepts used in the control of the internal degrees of freedom. We then turn to the control of the external motion of an atom using electromagnetic field. We show how one can trap atoms (section 3) and cool them (section 4). Finally, we review in section 5 a few important applications of cold atoms.

2 Manipulation of the internal state of an atom

2.1 Angular momentum of atoms and photons.

Atoms are like spinning tops. They have an internal angular momentum $\boldsymbol{J}$. As most physical quantities, the projection J_z of $\boldsymbol{J}$ along the z-axis is quantized : $J_z = M\hbar$, where $\hbar = h/(2\pi)$ and where M is an integer or half-integer, positive or negative.

Consider for example the simple case of a spin 1/2 atom. The *quantum number* J characterizing the angular momentum is $J = 1/2$ and there are two possible values of the magnetic quantum number M :

$$M = +1/2 \ : \ \text{Spin up} \ \Uparrow \qquad\qquad M = -1/2 \ : \ \text{Spin down} \ \Downarrow$$

At room temperature and in a low magnetic field, the Boltzmann factor $\exp(-\Delta E \,/\, k_B T)$ corresponding to the energy splitting ΔE between the two states is very close to 1 (k_B is

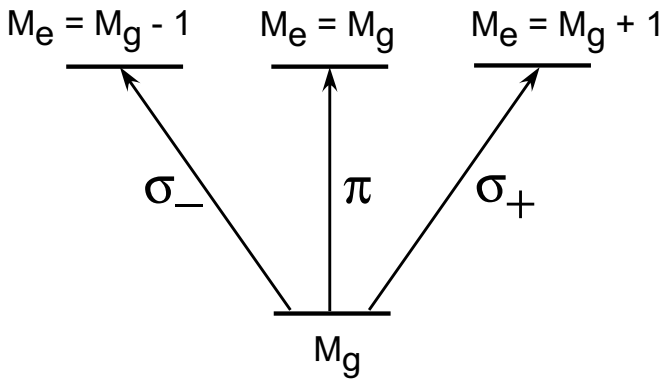

FIGURE 2: Polarization selection rules resulting from the conservation of the total angular momentum after the absorption of a photon by an atom.

the Boltzmann constant). The population of the two spin states are nearly equal and the spin polarization is negligible.

Photons have also an angular momentum J_z which depends on their polarization (see Figure 1). For a right circular polarization with respect to the z axis (called σ_+ polarization), $J_z = +\hbar$. For a left circular polarization with respect to the z axis (called σ_- polarization), $J_z = -\hbar$. Finally, for a linear polarization parallel to the z axis (called π polarization), $J_z = 0$.

Polarization selection rules. When an atom absorbs a photon, it gains the angular momentum of the absorbed photon and its magnetic quantum number changes from M_g to M_e. The change $(M_e - M_g)\,\hbar$ of the atomic angular momentum must be equal to the angular momentum of the absorbed photon. It follows that $M_e - M_g$ must be equal to $+1$ after the absorption of a σ_+-polarized photon, to -1 after the absorption of a σ_--polarized photon, to 0 after the absorption of a π-polarized photon. These *polarization selection rules* result from the conservation of the total angular momentum and express the clear connection which exists between the variation $M_e - M_g$ of the magnetic quantum number of an atom absorbing a photon and the polarization of this photon (see Figure 2).

2.2 Optical pumping

Optical pumping, developed in the early nineteen fifties by Alfred Kastler and Jean Brossel is a first example of manipulation of atoms with light. To explain optical pumping, let us consider the simple case of a transition connecting a ground state g with an angular momentum $J_g = 1/2$ to an excited state e with an angular momentum $J_e = 1/2$, so that there are two ground state Zeeman sublevels $g_{+1/2}$ and $g_{-1/2}$ and two excited Zeeman sublevels $e_{+1/2}$ and $e_{-1/2}$ (see Figure 3). If one excites such an atom with σ_+-polarized light, one drives only the transition $g_{-1/2} \rightarrow e_{+1/2}$ because this is the only transition

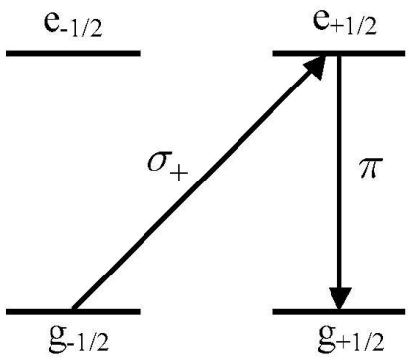

FIGURE 3: Principle of optical pumping for a $1/2 \rightarrow 1/2$ transition. Atoms are transferred from $g_{-1/2}$ to $g_{+1/2}$ by an *optical pumping cycle* which consists of an absorption of a σ_+-polarized photon followed by the spontaneous emission of a π-polarized photon.

corresponding to the selection rule $M_e - M_g = 1$ associated to a σ_+-excitation (see § 2.1). Once the atom has been excited in $e_{+1/2}$, it can fall back by spontaneous emission either in $g_{-1/2}$, in which case it can repeat the same cycle, or in $g_{+1/2}$ by emission of a π-polarized photon. In the last case, the atom remains trapped in $g_{+1/2}$ because there is no σ_+ transition starting from $g_{+1/2}$ (see Figure 3). This gives rise to an optical pumping cycle transferring atoms from $g_{-1/2}$ to $g_{+1/2}$ through $e_{+1/2}$. During such an absorption-spontaneous emission cycle, the angular momentum of the impinging photons has been transferred to the atoms which thus become polarized.

It clearly appears in Figure 3 that atoms absorb resonant light only if they are in $g_{-1/2}$. If they are in $g_{+1/2}$, they cannot absorb light because there is no σ_+-transition starting from $g_{+1/2}$. This means that any transfer of atoms from $g_{+1/2}$ to $g_{-1/2}$ which would be induced by a resonant radio-frequency (RF) field or by a relaxation process can be detected by monitoring the amount of light absorbed with a σ_+-polarization.

A first interesting feature of these optical methods is that they provide a very efficient scheme for polarizing atoms at room temperature and in a low magnetic field. Secondly, they have a very high sensitivity. A single RF transition between the 2 ground state sublevels is detected by the subsequent absorption or emission of an optical photon and it is much easier to detect an optical photon than a RF photon because it has a much higher energy. At last, these optical methods allow one to study and to investigate non-equilibrium situations. Atoms are removed from their thermodynamic equilibrium by optical pumping. By observing the temporal variations of the absorbed or emitted light, one can study how the system returns to equilibrium.

Magnetic resonance imaging with optical pumping. Optical pumping has recently found an interesting application for imaging the human body. One prepares a sample of polarized gaseous helium 3, using optical pumping with a laser. This gas is inhaled

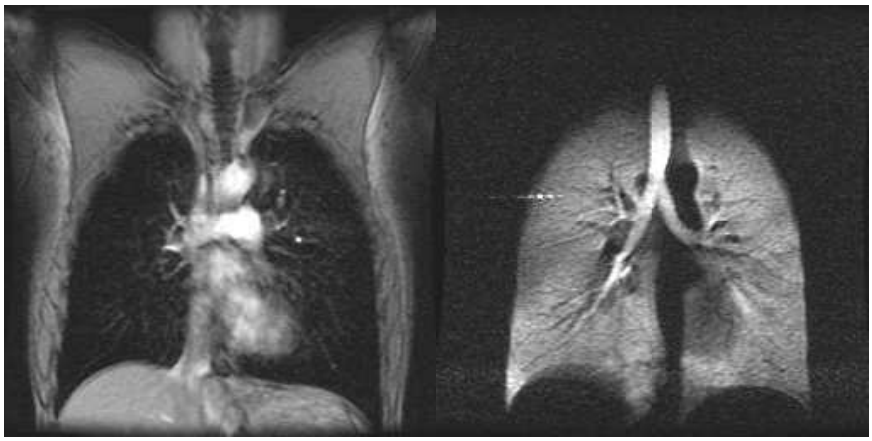

FIGURE 4: Magnetic Resonance Imaging of the chest of a patient. Left: image obtained with ordinary proton-based resonance. Right: image obtained with gaseous helium-based resonance. The patient has inhaled a mixture of air and helium 3, and the latter has been polarized using optical pumping (photographs: courtesy of Physics World. Figure taken from the article of G. Allan Johnson, Laurence Hedlund and James MacFall, November 1998).

by patients (this is harmless!) and it is used to perform magnetic resonance imaging (MRI) of the cavities in their lungs (Figure 4). Current proton-based MRI only provides information on solid or liquid parts of the human body like the muscles, the brain, or the blood (left part of Figure 4). The use of gaseous polarized helium with high degrees of spin polarization provides MRI signals strong enough to be detected even with a system as dilute as a gas. These signals allow internal spaces of the body, like the cavities of the lung, to be visualized at unprecedented resolutions (right part of Figure 4). The use of this polarized gas is a promising tool for improving our understanding of lung physiology and function.

2.3 Light broadening and light shifts

The interaction of an atom with the electromagnetic field perturbs atomic energy levels. This perturbation exists even in the absence of any incident light beam, in the "vacuum" of photons. Atomic energy levels are shifted. The interpretation of this effect, discovered by Willis Lamb in 1947, has stimulated the development of Quantum Electrodynamics, which is the prototype of modern quantum field theories. It can be interpreted as due to "virtual" emissions and re-absorptions of photons by the atom. Atomic excited states are also broadened, the corresponding width Γ being called the natural width of the atomic excited state e. In fact, Γ is the rate at which an excited atom spontaneously emits a photon and falls in the ground state g. It can be also written $\Gamma = 1/\tau_R$, where τ_R is called

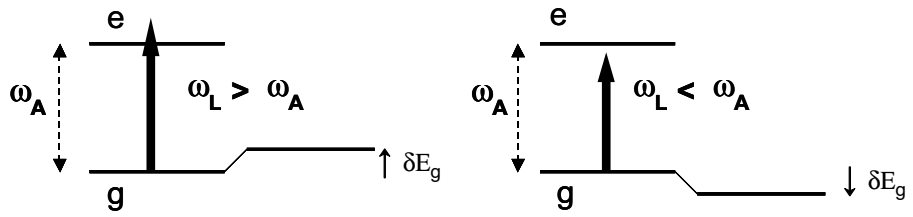

FIGURE 5: Light shift of the ground state g of an atom produced by a non resonant light excitation detuned to the red side of the atomic transition (right part of the figure) or to the blue side (left part of the figure).

the radiative lifetime of the excited state, *i.e.* the mean time after which an atom leaves the excited state by spontaneous emission.

A light irradiation introduces another perturbation for the ground state of an atom, which can be also described, at low enough intensities, as a broadening Γ' and a shift δE_g of the atomic ground state g. Both quantities depend on the light intensity I_L and on the detuning $\Delta = \omega_L - \omega_A$ between the light frequency ω_L and the atomic frequency ω_A. The broadening Γ' is the rate at which photons are scattered from the incident beam by the atom. The shift δE_g is the energy displacement of the ground level, as a result of virtual absorptions and stimulated emissions of photons by the atom within the light beam mode; it is called light-shift or AC Stark shift. It was predicted and observed by Jean-Pierre Barrat and one of the authors of this article (C.C-T) in the early nineteen sixties. At resonance ($\Delta = 0$), $\delta E_g = 0$ and Γ' takes its maximum value. For large enough detunings, δE_g is much larger than $\hbar\Gamma'$. One can show that δE_g is then proportional to I_L/Δ. The light shift produced by a non resonant light irradiation is thus proportional to the light intensity and inversely proportional to the detuning. In particular, it has the same sign as the detuning (see Figure 5).

3 Electromagnetic forces and trapping

The most well known action of an electromagnetic field on a particle is the Lorentz force. Consider a particle with charge q moving with velocity $\boldsymbol{v}$ in an electric field $\boldsymbol{E}$ and a magnetic field $\boldsymbol{B}$. The resulting force $\boldsymbol{F} = q(\boldsymbol{E} + \boldsymbol{v} \times \boldsymbol{B})$ is used in all electronic devices. For neutral particles, such as neutrons, atoms or molecules, the Lorentz force is zero. However one can still act on these particles using the interaction of their electric dipole moment $\boldsymbol{D}$ or magnetic dipole moment $\boldsymbol{\mu}$ with a gradient of electric or magnetic field. The interaction energy of the dipole with the field is $-\boldsymbol{D} \cdot \boldsymbol{E}$ or $-\boldsymbol{\mu} \cdot \boldsymbol{B}$, and it constitutes a potential energy for the motion of the center of mass of the particle. Depending on the relative orientation between the dipole and the field, the resulting force is directed towards large or small field regions.

In the following we shall first address the possibility to trap charged particles with electromagnetic fields (§ 3.1). We shall then turn to neutral particles and we shall discuss separately the case of magnetic forces (§ 3.2) and electric (§ 3.3) forces. The physical concepts involved are quite different since one deals with a permanent dipole moment in the first case, and an induced moment in the latter. We shall finally turn to the radiation pressure force (§ 3.4), and present two spectacular applications of this force to atom manipulation: the deceleration of an atomic beam and the magneto-optical trap.

3.1 Trapping of charged particles

At first sight, the simplest trap for charged particles should consist in a pure electrostatic field $\boldsymbol{E}(\boldsymbol{r})$ such that the electrostatic force $\boldsymbol{F} = q\boldsymbol{E}$ in the vicinity of a given point O would be a restoring force. This is unfortunately forbidden by the Gauss equation for electrostatics $\boldsymbol{\nabla} \cdot \boldsymbol{E} = 0$, which entails $\boldsymbol{\nabla} \cdot \boldsymbol{F} = 0$. This result, which makes it impossible to have a force pointing inwards a sphere centered in any point O, is known as the Earnshaw theorem. We present hereafter two possibilities to circumvent this theorem. The first one takes advantage of the time dependence of the applied electric field. The second possibility uses a combination of electric and magnetic fields.

The Paul trap. The principle of this trap, invented by Wolfgang Paul, consists in placing the particle to be trapped in an electric field which is rapidly oscillating at frequency Ω: $\boldsymbol{E}(\boldsymbol{r}, t) = \boldsymbol{\mathcal{E}}(\boldsymbol{r})\ \cos(\Omega t)$, the amplitude $\mathcal{E}(\boldsymbol{r})$ vanishing in the center of the trap O. The motion of the particle can then be decomposed in a fast oscillation at frequency Ω (the micro-motion) superimposed with a motion with a slower characteristic frequency. After average over a time period $2\pi/\Omega$, the kinetic energy associated with the micro-motion is $U(\boldsymbol{r}) = q^2\,\mathcal{E}^2(\boldsymbol{r})/(4m\Omega^2)$. This kinetic energy plays the role of a potential energy for the slow motion. It is null in O, since $\mathcal{E}$ vanishes in this point, and positive everywhere else. One thus achieves in this way a potential well centered in O, which confines the particle. The consistency of the above treatment is ensured by choosing the field amplitude $\mathcal{E}$ such that the oscillation frequency of the particle in the potential $U(\boldsymbol{r})$ is indeed much smaller than the fast frequency Ω.

The Penning trap. The Penning trap is formed by the superposition of a quadrupole electrostatic potential $V(\boldsymbol{r})$ and a uniform magnetic field $\boldsymbol{B}$ parallel to the z axis (Figure 6, left). The electrostatic potential ensures trapping along the z direction, and it expels the particle in the perpendicular xy plane; it can be written $V(\boldsymbol{r}) = \kappa(2z^2 - x^2 - y^2)$ where κ is a constant. The Newton equations of motion for the particle are linear in $\boldsymbol{r}$ and $\boldsymbol{v}$; hence they can be solved exactly. For $qB > (8\kappa m)^{1/2}$, one finds that the motion in the xy plane is stabilized by the magnetic field, while the trapping along the z axis by the quadrupole electric field is not affected. One thus achieves a stable three-dimensional confinement of the particles.

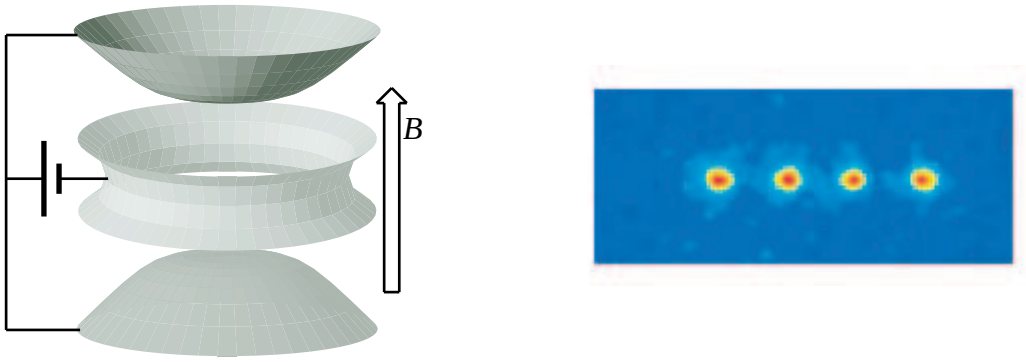

FIGURE 6: Trapping charged particles. Left: scheme of electrodes used in a Penning trap, with a vertical magnetic field. Right: chain of 4 calcium ions confined in a linear Paul trap; the distance between two ions is 15 μm (photograph by courtesy of Rainer Blatt, Innsbruck).

Applications. Both Paul and Penning traps are extensively used in modern physics. They are often associated with an efficient cooling of the particles using either a quasi-resonant laser light (see § 4.3) or a resonant coupling with a damped electrical circuit. They allow a precise measurement of the cyclotron frequency qB/m of the trapped particle. By comparing this ratio for a single electron and a single positron, or for a single proton and a single antiproton, Penning traps have allowed tests of the symmetry between matter and anti-matter with a unprecedented precision. One can also use this trap to accurately measure the gyromagnetic ratio of a particle, *i.e.* the ratio between the cyclotron frequency and the Larmor frequency, characterizing the evolution of the magnetic moment. Using a single trapped electron, Hans Dehmelt and his group have used this system to test quantum electrodynamics at the 10^{-12} level of accuracy. Single ions trapped in Penning or Paul traps are used for ultra-high resolution spectroscopy and metrology. It is also possible to trap large assemblies of ions in these traps and to study in great detail the macroscopic behavior of these plasmas. Last but not least, a string of a few ions trapped in a Paul trap is considered as a very promising system to implement the basic concepts of the new field of quantum information (Figure 6, right).

3.2 Magnetic dipole force

One of the most celebrated experiments performed in the early days of Quantum Mechanics is the Stern-Gerlach experiment. In that experiment performed in 1921, a beam of silver atoms was sent in a region with a large magnetic gradient. Otto Stern and Walther Gerlach observed that the beam was split into two components, one being deflected towards the region of large magnetic field, the other one being deflected away from this region.

The modern interpretation of this experiment is straightforward within the framework that we outlined in section 2. The silver atoms have a spin $J = 1/2$, and they possess a magnetic moment $\boldsymbol{\mu}$ proportional to their angular momentum $\boldsymbol{\mu} = \gamma \boldsymbol{J}$ where γ is a

constant. Therefore the projection of the magnetic moment along the axis of the magnetic field can take only two values, $\pm\hbar\gamma/2$, corresponding to an orientation of $\boldsymbol{\mu}$ either parallel or anti-parallel to $\boldsymbol{B}$. The magnetic interaction energy is then $-\boldsymbol{\mu}\cdot\boldsymbol{B} = \mp\mu B$. Atoms with $\boldsymbol{\mu}$ parallel to $\boldsymbol{B}$ (energy $-\mu B$) are attracted by the high field region, and atoms with $\boldsymbol{\mu}$ anti-parallel to $\boldsymbol{B}$ are deflected towards the low field region. The magnetic force can be quite large in practice. Consider a hydrogen atom in its ground state; μ is the Bohr magneton, of the order of 10^{-23} J/T. In the vicinity of a strong permanent magnet, the gradient is ~ 10 T/m, hence a force 6000 times larger than gravity.

Magnetic trapping of neutral atoms. The magnetic force is now widely used to trap neutral particles such as atoms, neutrons or molecules. Static magnetic traps are centered around a point O where the amplitude B of the magnetic field is minimum. Atoms prepared with a magnetic moment $\boldsymbol{\mu}$ antiparallel with $\boldsymbol{B}$ (*low field seekers*) have a magnetic energy $\mu B(\boldsymbol{r})$ and they feel a restoring force towards O. On the contrary, it is not possible to achieve a local maximum of B (except on the surface of a conductor). Therefore one cannot form a stable magnetic trap for *high field seekers*, *i.e.* atoms with $\boldsymbol{\mu}$ parallel to $\boldsymbol{B}$.

The first magnetic trap for neutrons has been demonstrated by Wolfgang Paul and his group in 1975. William Phillips and his team observed the first magnetically trapped atomic gas in 1985. Nowadays the most commonly used magnetic trap is the Ioffe-Pritchard trap, which ensures confinement around a location O where the field $\boldsymbol{B}_0$ is non zero, typically from 0.1 to 1 mT (Figure 7). This ensures that the Larmor frequency characterizing the evolution of $\boldsymbol{\mu}$ is large, of the order of 1 to 10 MHz. Since the oscillation frequency of the atom in the trap is usually much smaller (a few hundred Hz only), this allows the magnetic moment $\boldsymbol{\mu}$ to adjust adiabatically to the direction of $\boldsymbol{B}$ during the displacement of the atom in the trap: an atom initially prepared in a low field seeking state will remain in this state during the course of its evolution.

Magnetic traps are simple to design and to build, and atoms can be stored for long durations (several minutes) at very low temperatures (microkelvin), without any appreciable heating. In fact the lifetime of an atom trapped in a magnetic trap is mostly determined by the quality of the vacuum in the chamber containing the trap. Indeed, the trap depth is relatively low so that a collision with a molecule from the background gas ejects the atom out of the trap. Magnetic traps have played a key role in the achievement of Bose-Einstein condensation with atomic gases. They are also used to trap atomic fermionic species and molecules.

3.3 Electric dipole force

Permanent dipole moment: molecules. For a system with a permanent electric dipole $\boldsymbol{D}$ such as a hetero-molecule (CO, NH_3, H_2O), one can transpose the reasoning given above for a magnetic dipole. When the molecule is placed in an electric field,

FIGURE 7: Magnetic trapping of neutral atoms. Left: Ioffe-Pritchard trap, consisting in 4 linear conductors and two circular coils. The arrows indicate the current direction in each conductor. The modulus of the magnetic field has a non zero local minimum at the center of symmetry O of the system. Atoms with a magnetic moment antiparallel to the local magnetic field are confined around O. Right: photograph of 10^7 cesium atoms confined in a Ioffe-Pritchard trap. The image of the cigar-shaped atom cloud has been obtained by recording the absorption of a short resonant laser pulse and making the image of the shadow of the atom cloud onto a CCD camera. The temperature is of the order of 10 microkelvins (photograph: ENS).

the projection D_z of its dipole moment on the electric field direction is quantized. It can take $2J+1$ values, where J is the angular momentum of the molecular state under consideration; the electrostatic energy $-\boldsymbol{D}\cdot\boldsymbol{E} = -D_z E$ give rise to $2J+1$ potential energy surfaces. If the molecular beam propagates in a region where the electric field is inhomogeneous, a different force corresponds to each surface and the beam is split into $2J+1$ components.

This electric dipole force is used in many devices, such as the ammonia maser where it is at the basis of the preparation of the population inversion. A recent spectacular application of this force has been developed in the group of Gerard Meijer in Nijmegen. It consists in decelerating a pulsed beam of molecules using electric field gradients. The beam is sent in a region of increasing field, so that molecules with $\boldsymbol{D}$ antiparallel to $\boldsymbol{E}$ are slowed down. With a maximum field of 10^7 V/m the kinetic energy decrease is of the order of $k_B \times 1$ K. The electric field is then switched off as soon as the molecule pulse has reached the location where this field is large. Using a carefully designed stack of electrodes, one repeats this operation a large number of times over the total length of the beam (typically 1 meter) and the molecule pulse can be brought nearly at rest.

Induced dipole moment: atoms. For atoms, the permanent dipole moment is null, as a consequence of the symmetry of the physical interactions at the origin of the atom stability. However it is still possible to act on them using an electric field gradient, through an *induced* electric dipole moment. When an atom is placed in a static electric field $\boldsymbol{E}$, it acquires a dipole moment $\boldsymbol{D} = \alpha_0 \boldsymbol{E}$, where α_0 is the static polarizability. For simplicity we shall assume here that α_0 is a scalar, although it may also have a tensorial part.

The potential energy of an atom in an electric field is $W = -\alpha_0 E^2/2$ and the corresponding force is $\boldsymbol{F} = -\boldsymbol{\nabla} W = \alpha_0 \boldsymbol{\nabla}(E^2)/2$. For an atom in its ground state g, α_0 is positive. Therefore the atom is always attracted to the regions where the electric field is the largest. The potential energy W is nothing but the shift of the relevant atomic internal state induced by the electric field. It is calculated here at the second order of perturbation theory, assuming a linear response of the atom with respect to the field. We neglect here saturation effects, which is valid as long as the applied electric field is small compared with the inner field of the atom, created by the nucleus.

This analysis can be generalized to the case of a time-dependent electric field. Consider a field oscillating with the angular frequency ω_L. The static polarizability must then be replaced by the dynamic polarizability $\alpha(\omega_L)$. When ω_L is much smaller than the relevant atomic Bohr frequencies $\omega_{\rm A}$ of the atom, then $\alpha(\omega_L) \simeq \alpha_0$. This is the case in many experiments where one manipulates ground state alkali atoms (Bohr frequencies $\omega_{\rm A} \sim 3 \times 10^{15}$ s^{-1}) with very far detuned laser light, such as the radiation from a CO_2 laser ($\omega_L \sim 2 \times 10^{14}$ s^{-1}).

Resonant dipole force. A very important practical case concerns an atom in its ground internal state, which is irradiated with a laser wave whose frequency ω_L is comparable with the atomic Bohr frequency $\omega_{\rm A}$ corresponding to the resonance transition $g \leftrightarrow e$. In this case the dipole potential $W(\boldsymbol{r}) = -\alpha(\omega_L)\, E^2(\boldsymbol{r})/2$ is nothing but the light shift δE_g of the ground state that we have derived in § 2.3. We recall that the sign of the light shift, hence the direction of the dipole force, depends on the sign of the detuning to resonance $\Delta = \omega_L - \omega_{\rm A}$. When Δ is negative, the result is qualitatively the same as for a static field; the atom is attracted to the region of large laser intensities. On the contrary, when Δ is positive, the force on the atom tends to push it away from high intensity regions. The dipole force is non zero only if the light intensity is spatially inhomogeneous. One can show that it can be interpreted as resulting from a redistribution of photons between the various plane waves forming the laser wave in absorption-stimulated emission cycles.

When the laser intensity is increased to a large value, the atom spends a significant time in the excited internal state e. In this case the preceding expression of the dipole potential must be modified. A convenient point of view on the system is obtained through the *dressed atom* formalism, in which one deals with the energy levels of the combined system "atom + laser photons". Two types of dressed states are found, connecting respectively to the ground and to the excited atomic states when the laser intensity tends to zero. The forces associated to the two dressed states are opposite. Since spontaneous emission processes cause random jumps between the two types of dressed states, the atomic motion is stochastic, with an instantaneous force oscillating back and forth between two opposite values in a random way. Such a dressed atom picture provides a simple interpretation of the mean value and of the fluctuations of dipole forces.

Dipole traps for neutral atoms. One of the most spectacular uses of the resonant dipole force is the possibility to trap atoms around local maxima or minima of the laser intensity. The first laser trap has been demonstrated in 1985 at Bell Labs, in the group of Steven Chu and Arthur Ashkin, using a single focused travelling laser wave. Atoms were accumulated at the vicinity of the focal point of the light wave. Later on, several other traps have been investigated, such as hollow tubes used as atom guides. The research on dipole traps has led to another spectacular development, *optical tweezers*. The object being trapped is not anymore a single atom, but a micron-size dielectric sphere. It can be attached to objects of biological interest, such as a DNA molecule, and it allows the microscopic manipulation of these objects.

Optical lattices. Optical lattices are formed by the periodic modulation of the light intensity in a laser standing wave. Depending on the sign of the detuning Δ, the atoms accumulate at the nodes or the antinodes of the standing wave (Figure 8, left). Optical lattices, initially studied by the groups of Gilbert Grynberg and William Phillips, have led to several spectacular developments, both from theoretical and experimental points of view. The tunnelling between adjacent wells plays a significant role in the dynamics of the atoms, and these lattices constitute model systems for studying quantum transport in a periodic potential. As an example, the group of Christophe Salomon has shown that atoms submitted to a constant force in addition to the lattice force undergo periodic Bloch oscillations, instead of being uniformly accelerated as in absence of a lattice. Also, the team of Theodor Hänsch and Immanuel Bloch has observed the superfluid-insulator Mott transition for an ultra-cold gas placed in an optical lattice. The superfluid phase corresponds to a Bose-Einstein condensate, where each atom is delocalized over the whole lattice. The isolating phase is obtained by increasing the lattice depth so that the tunnelling between adjacent wells is reduced. The repulsion between atoms then favors a situation where the number of atoms at each lattice node is fixed.

Atom mirrors. For a positive detuning of the laser wave with respect to the atomic frequency, the dipole force repels the atoms from the high intensity region. It is thus possible to create a potential barrier on which the atoms can be elastically reflected. Following a suggestion by Richard Cook and Richard Hill, several groups have used a evanescent wave propagating at the surface of a glass prism to form an atom mirror (Figure 8, right). The incident atoms arrive on the vacuum side and feel the repulsive dipole force as they enter the evanescent wave. If their incident kinetic energy is smaller than the potential barrier created by the light, atoms turn back before touching the glass.

In practice, with a laser intensity of 1 Watt focused on a surface of the order of 1 mm^2, an atom can be reflected if the component of its velocity normal to the mirror is lower than a few meters per second. Such atomic mirrors are therefore well suited for manipulating laser cooled atoms (see § 4). They constitute very useful components for the development of atom optics. Using a curved dielectric surface, one can focus or defocus an atomic beam.

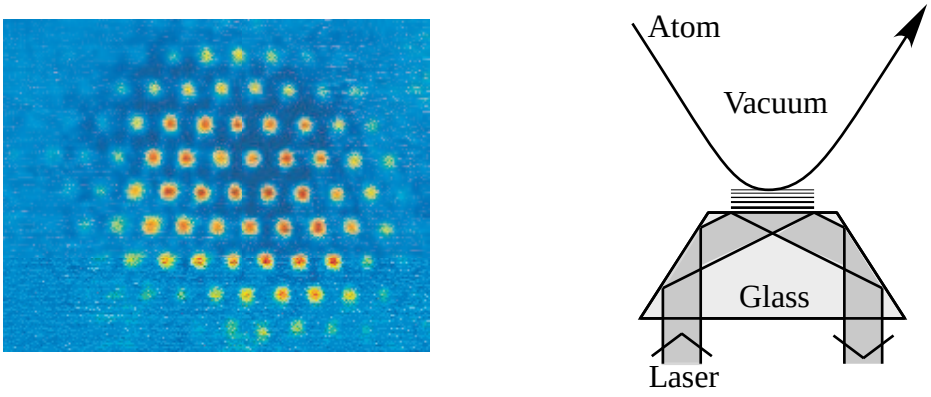

FIGURE 8: Manipulation of atoms using the resonant dipole force. Left: photograph of cesium atoms captured in a hexagonal optical lattice with a period of 29 micrometers. Each spot contains 10^4 atoms (picture: courtesy of C. Salomon, ENS Paris). Right: atom mirror formed by an evanescent wave propagating at the surface of a glass prism. For a positive detuning Δ of the laser beam with respect to the atomic resonance, the atoms are repelled from the high intensity region. If their incident kinetic energy is low enough, they bounce elastically on the light sheet without touching the glass surface.

Using a evanescent wave whose intensity is modulated in time, one realizes a vibrating mirror. The corresponding modulated Doppler shift introduces a frequency modulation of the reflected de Broglie wave.

3.4 The radiation pressure force

Recoil of an atom emitting or absorbing a photon. Consider an atom in an excited electronic state e, with its center of mass initially at rest. At a certain time, the atom emits a photon and drops to its electronic ground state g. The total momentum of the system is initially zero and it is conserved throughout the whole process. Therefore in the final state, since the emitted photon carries away the momentum $\hbar\boldsymbol{k}$, the atom recoils with momentum $-\hbar\boldsymbol{k}$. This recoil phenomenon also occurs when an atom absorbs a photon. Consider the atom in its ground state g and its center of mass initially at rest; suppose that a photon with wave vector $\boldsymbol{k}$ is sent on this atom. If the atom absorbs the photon, it jumps to the excited state and it recoils with the momentum $\hbar\boldsymbol{k}$.

To the change $\hbar k$ of the atom momentum corresponds a change $v_{\rm rec} = \hbar k/m$ of the atom velocity, where m is the atom mass. For an hydrogen atom absorbing or emitting a photon on the Lyman α line (2p $\rightarrow$ 1s transition), this recoil velocity is 3 m/s. For a sodium atom, a photon emitted or absorbed on its resonance line (wavelength 590 nm) corresponds to a velocity change of $v_{\rm rec} = 3$ cm/s. These are very low velocities compared to those of atoms or molecules at room temperature, which are on the order of several hundreds of meters per second. This explains why the velocity changes due to recoil effects have been most of the time neglected in the past. However, as we see below, the

repetition of these velocity changes can lead to large forces.

The radiation pressure in a resonant light wave. Consider an atom placed in a travelling laser wave with wave vector $\boldsymbol{k}$. We assume that the laser frequency ω_L is resonant with the atomic transition $g \leftrightarrow e$ at frequency ω_A. The atom then undergoes a succession of *fluorescence cycles*. The atom initially in its ground state absorbs a photon from the laser beam and gains the momentum $\hbar\boldsymbol{k}$. After a time of the order of the radiative lifetime τ_R of the electronic excited state e, the atom decays back to the ground state by emitting spontaneously a photon. The direction of emission of this fluorescence photon is random; the symmetry properties of spontaneous emission are such that the probabilities of the photon being emitted in two opposite directions are equal. Therefore the momentum change in a spontaneous emission averages out to zero. It follows that in a fluorescence cycle, the average variation of the atomic velocity is only related to the absorption process and it is equal to $\hbar\boldsymbol{k}/m$.

The repetition rate of these cycles is only limited by the lifetime τ_R of the excited state e. Since τ_R is on the order of 10^{-8} s, about 10^8 (one hundred million!) fluorescence cycles can take place per second. During each cycle, the velocity of the atom changes on the average by an amount $v_{\rm rec} \sim 1$ cm/s. Being repeated 100 millions times per second, this produces a velocity change per second 100 millions times larger than the recoil velocity, corresponding to an acceleration or a deceleration on the order of 10^6 m/s^2. Radiation pressure forces are therefore 10^5 times larger than the gravity force!

Stopping an atomic beam. This considerable radiation pressure force makes it possible to stop an atomic beam. Consider a sodium atomic beam coming out of an oven at a temperature of 500 K, corresponding to an average speed of 1 km/s. We irradiate this atomic beam by a counter-propagating resonant laser beam, so that the radiation pressure force slows the atoms down. If the available distance is large enough, the atoms may even stop and return in the opposite direction: an atom with an initial velocity 1 km/s and submitted to a deceleration of 10^6 m/s^2 is brought at rest in one millisecond. During this deceleration time it travels over 50 cm only, which makes such an atom decelerator very practicable (Figure 9, left).

A complication in the deceleration process originates from the Doppler effect. As the atom velocity v changes, the laser frequency in the atom frame $\tilde{\omega}_L = \omega_L - kv$ also changes and the resonance condition $\tilde{\omega}_L = \omega_A$ is not fulfilled anymore. In order to circumvent this problem, several solutions have been proposed and demonstrated: use of an inhomogenous magnetic field so that the Zeeman effect also changes the atomic resonance frequency ω_A as the atom progresses in the decelerator, chirping of the laser frequency during the deceleration process, use of a broadband laser, etc. The first atoms stopped by radiation pressure have been observed in 1984 in the groups of William Phillips and John Hall.

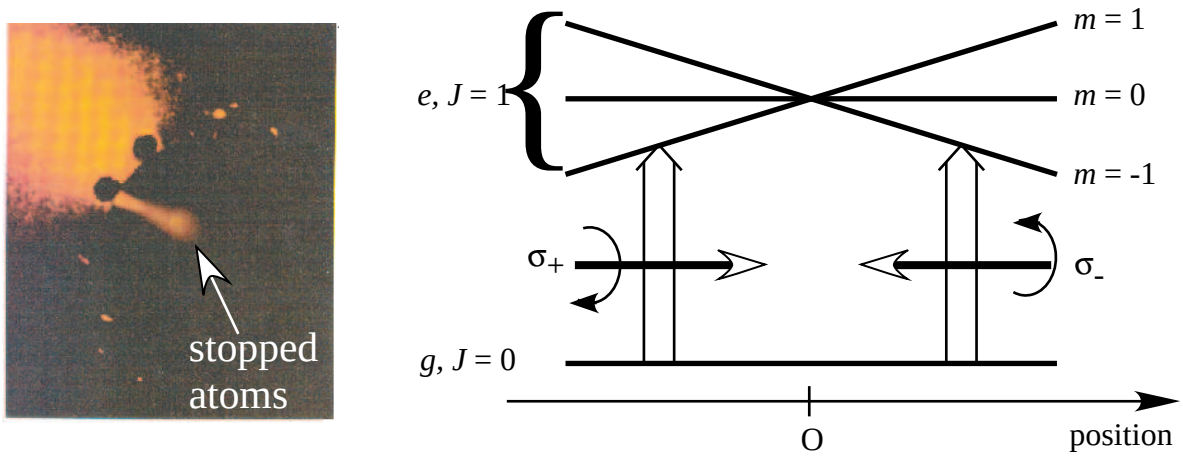

FIGURE 9: Manipulation of atoms using the radiation pressure force. Left: photograph of a beam of sodium atoms stopped by the radiation pressure of a counter-propagating laser beam (photograph: courtesy of W. D. Phillips, NIST Gaithersburg). Right: principle of the magneto-optical trap. The two counter-propagating laser waves have the same intensity and the same frequency, and they are respectively σ_+ and σ_- polarized. In presence of a magnetic field, the balance between the two radiation pressure forces is broken; using a gradient of magnetic field, one achieves a situation where atoms feel a restoring force to the center O.

The magneto-optical trap. The radiation pressure force can be used to trap quite efficiently neutral atoms. The trap is based upon the imbalance between the opposite radiation pressure forces created by two counter-propagating laser waves. The imbalance is made position dependent though a spatially dependent Zeeman shift produced by a magnetic field gradient. The principle of the trap takes advantage of both the linear and angular momenta carried by the photons. For simplicity we present its principle for a one-dimensional configuration, as first suggested by one of the authors of this article (J.D.) in 1986; we assume that the angular momenta of the ground g and excited e internal levels involved in the trapping are respectively $J_g = 0$ and $J_e = 1$ (Figure 9, right). The two counter-propagating waves have the same negative detuning Δ ($\omega_L < \omega_A$) and they have opposite circular polarizations; they are thus in resonance with the atom at different places. At the center O of the trap, the magnetic field is zero. By symmetry the two radiation pressure forces have the same magnitude and opposite directions. They balance each other and an atom in O feels no net force. Consider now an atom at the left of O. The laser wave coming from the left, which is σ_+-polarized, is closer to resonance with the allowed transition $g \leftrightarrow e, m = +1$ than for an atom in O. The radiation pressure created by this wave is therefore increased with respect to its value in O. Conversely, the radiation pressure force created by the wave coming from the right is decreased with respect to O. Indeed the wave is σ_- polarized and it is further from resonance with the transition $g \leftrightarrow e, m = -1$ than it is in O. Therefore the net force for an atom at the left of O is pointing towards O. For an atom located at the right of O, the reverse

phenomenon occurs: the radiation pressure force created by the wave coming from the right now dominates, so that the resulting force also points towards O. One therefore achieves a stable trapping around O.

Such a scheme can be extended to three dimensions, as first demonstrated in a collaboration between the groups of M.I.T. and Bell Labs, and it leads to a robust, large and deep trap called *magneto-optical trap*. It has a large velocity capture range and it can be used for trapping atoms in a cell filled with a low pressure vapor, as shown by the JILA Boulder group. Furthermore the non zero value of the detuning provides cooling of the trapped atoms, along the lines that will be discussed in the next section (§ 4).

4 Cooling of atoms

The velocity distribution of an ensemble of atoms is characterized by the mean velocity and the velocity dispersion around the mean value. In physics, temperature is associated with this velocity spread, *i.e.* with the disordered motion of the atoms. The hotter the temperature of the medium, the higher the velocity dispersion of its constituents. For cooling a system, this velocity spread has to be reduced.

4.1 Doppler cooling

The simplest cooling scheme uses the Doppler effect and was first suggested in 1975 by Theodor Hänsch and Arthur Schawlow for free atoms and by David Wineland and Hans Dehmelt for trapped ions. The concept is basically simple; we explain it for free atoms, in which case it is very reminiscent of the principle of the magneto-optical trap that we just discussed. Consider an atom which is irradiated by two counter-propagating laser waves (Figure 10). These two laser waves have the same intensity and the same frequency ω_L slightly detuned below the atomic frequency ω_A. For an atom at rest with zero velocity, there is no Doppler effect. The two laser waves have then the same apparent frequency. The forces being exerted have the same value with opposite signs, they balance each other and no net force is exerted on the atom. For an atom moving to the right with a velocity v, the frequency of the counter-propagating beam seems higher because of the Doppler effect. The wave gets closer to resonance, more photons are absorbed and the force created by this beam increases. Conversely the apparent frequency of the co-propagating wave is reduced because of Doppler effect and gets farther from resonance. Less photons are absorbed and the force decreases. For a moving atom, the two radiation pressure forces no longer balance each other. The force opposite to the atomic velocity finally prevails and the atom is thus submitted to a non-zero net force opposing its velocity. For a small velocity v, this net force can be written as $F = -\alpha v$ where α is a friction coefficient. The atomic velocity is damped out by this force and tends to zero, as if the atom was moving in a sticky medium. This laser configuration is called an *optical molasses*.

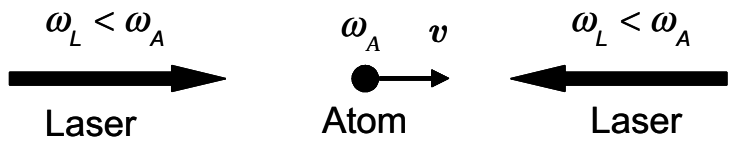

FIGURE 10: Doppler cooling in 1D, resulting from the Doppler induced imbalance between the radiation pressure forces of two counterpropagating laser waves. The laser detuning is negative ($\omega_L < \omega_A$).

Limit of Doppler cooling. The Doppler friction responsible for the cooling is necessarily accompanied by fluctuations due to the fluorescence photons which are spontaneously emitted in random directions and at random times. Each emission process communicate to the atom a random recoil momentum $\hbar k$, responsible for a momentum diffusion described by a diffusion coefficient D. As in usual Brownian motion, competition between friction and diffusion leads to a steady-state, with an equilibrium temperature proportional to D/α. A detailed analysis shows that the equilibrium temperature obtained with such a scheme is always larger than a certain limit $T_{\rm D}$, called the Doppler limit. This limit is given by $k_B T_{\rm D} = \hbar\Gamma/2$, where Γ is the natural width of the excited state. It is reached for a detuning $\Delta = \omega_L - \omega_A = -\Gamma/2$, and its value is on the order of 100 μK for alkali atoms. In fact, when the measurements became precise enough, the group of William Phillips showed that the temperature in optical molasses was much lower than expected. This indicated that other laser cooling mechanisms, more powerful than Doppler cooling, are operating. They were identified in 1998 by the Paris and Stanford groups. We describe in the next subsection one of them, the Sisyphus cooling mechanism, proposed by the authors of the present article.

4.2 Sisyphus cooling

The ground level g of most atoms, in particular alkali atoms, has a non zero angular momentum J_g. This level is thus composed of several Zeeman sublevels. Since the detuning used in laser cooling experiments is not large compared to Γ, both differential light shifts and optical pumping transitions exist for the various Zeeman sublevels of the ground state. Furthermore, the laser polarization and the laser intensity vary in general in space so that light shifts and optical pumping rates are position-dependent. We show now, with a simple one-dimensional example, how the combination of these various effects can lead to a very efficient cooling mechanism.

Consider the laser configuration of Figure 11, consisting of two counterpropagating plane waves along the z-axis, with orthogonal linear polarizations and with the same frequency and the same intensity. Because the phase shift between the two waves varies linearly with z, the polarization of the total field changes from σ^+ to σ^- and vice versa every $\lambda/4$. In between, it is elliptical or linear. We address here the simple case where

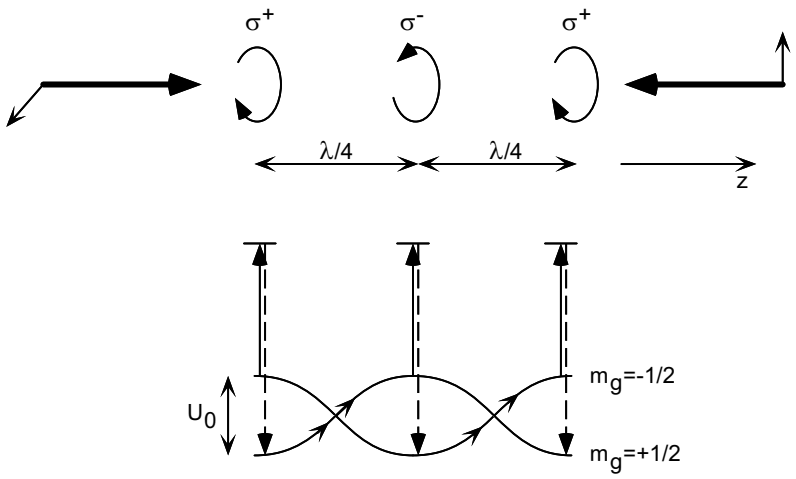

FIGURE 11: One dimensional Sisyphus cooling. The laser configuration is formed by two counterpropagating waves along the z axis with orthogonal linear polarizations. The polarization of the resulting field is spatially modulated with a period $\lambda/2$. For an atom with two ground Zeeman sublevels $M_g = \pm 1/2$, the spatial modulation of the laser polarization results in correlated spatial modulations of the light shifts of these two sublevels and of the optical pumping rates between them. Because of these correlations, a moving atom runs up potential hills more frequently than down.

the atomic ground state has an angular momentum $J_g = 1/2$. The two Zeeman sublevels $M_g = \pm 1/2$ undergo different light shifts, depending on the laser polarization, so that the Zeeman degeneracy in zero magnetic field is removed. This gives the energy diagram of Figure 11 showing spatial modulations of the Zeeman splitting between the two sublevels with a period $\lambda/2$.

If the detuning Δ is not very large compared to Γ, there are also real absorptions of photons by the atom followed by spontaneous emission, which give rise to optical pumping transfers between the two sublevels, whose direction depends on the polarization: $M_g = -1/2 \longrightarrow M_g = +1/2$ for a σ^+ polarization, $M_g = +1/2 \longrightarrow M_g = -1/2$ for a σ^- polarization. Here also, the spatial modulation of the laser polarization results in a spatial modulation of the optical pumping rates with a period $\lambda/2$.

The two spatial modulations of light shifts and optical pumping rates are of course correlated because they are due to the same cause, the spatial modulation of the light polarization. These correlations clearly appear in Figure 11. With the proper sign of the detuning, optical pumping always transfers atoms from the higher Zeeman sublevel to the lower one. Suppose now that the atom is moving to the right, starting from the bottom of a valley, for example in the state $M_g = +1/2$ at a place where the polarization is σ^+. Because of the finite value of the optical pumping time, there is a time lag between the dynamics of internal and external variables. The atom can climb up the potential hill before absorbing a photon. It then reaches the top of the hill where it has the maximum

probability to be optically pumped in the other sublevel, *i.e.* in the bottom of a valley, and so on.

Like Sisyphus in the Greek mythology, who was always rolling a stone up the slope, the atom is running up potential hills more frequently than down. When it climbs a potential hill, its kinetic energy is transformed into potential energy. Dissipation then occurs by light, since the spontaneously emitted photon has an energy higher than the absorbed laser photon. After each Sisyphus cycle, the total energy E of the atom decreases by an amount of the order of U_0, where U_0 is the depth of the optical potential wells of Figure 11. When E becomes smaller than U_0, the atom remains trapped in the potential wells.

Limits of Sisyphus cooling. The previous discussion shows that Sisyphus cooling leads to temperatures $T_{\rm Sis}$ such that $k_{\rm B}T_{\rm Sis} \simeq U_0$. We have seen above in subsection 2.3 that the light shift U_0 is proportional to I_L/Δ. Such a dependence of $T_{\rm Sis}$ on the laser intensity I_L and on the detuning Δ has been checked experimentally.

At low intensity, the light shift is much smaller than $\hbar\Gamma$. This explains why Sisyphus cooling leads to temperatures much lower than those achievable with Doppler cooling. One cannot however decrease the laser intensity to an arbitrarily low value. The previous discussion ignores the recoils due to the spontaneously emitted photons. Each recoil increases the kinetic energy of the atom by an amount on the order of $E_{\rm R}$, where

$$E_{\rm R} = \hbar^2 k^2/2M \tag{2}$$

is the recoil energy of an atom absorbing or emitting a single photon. When U_0 becomes on the order or smaller than $E_{\rm R}$, the cooling due to Sisyphus cooling becomes weaker than the heating due to the recoil, and Sisyphus cooling no longer works. This shows that the lowest temperatures which can be achieved with such a scheme are on the order of a few $E_{\rm R}/k_B$. This is on the order of a few microKelvins for heavy atoms such as rubidium or cesium. This result is confirmed by a full quantum theory of Sisyphus cooling and is in good agreement with experimental results.

For the optimal conditions of Sisyphus cooling, atoms become so cold that they get trapped in the few lowest quantum vibrational levels of each potential well, more precisely the lowest allowed energy bands of this periodic potential. This is an example of the optical lattices discussed in § 3.3. The steady-state corresponds to an anti-ferromagnetic order, since two adjacent potential wells correspond to opposite spin polarizations.

4.3 Sub-recoil cooling

In Doppler cooling and Sisyphus cooling, fluorescence cycles never cease. Since the random recoil $\hbar k$ communicated to the atom by the spontaneously emitted photons cannot be controlled, it seems impossible to reduce the atomic momentum spread δp below a value corresponding to the photon momentum $\hbar k$. The condition $\delta p = \hbar k$ defines the *single*

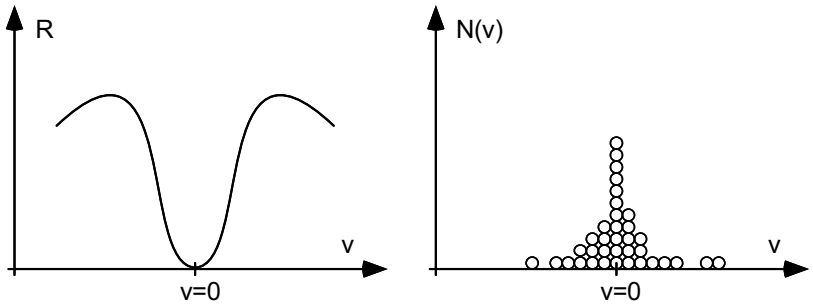

FIGURE 12: Sub-recoil cooling. The random walk in velocity space is characterized by a jump rate R vanishing in $v = 0$. As a result, atoms which fall in a small interval around $v = 0$ remain trapped there for a long time and accumulate.

photon recoil limit, the effective recoil temperature being set as $k_B T_R/2 = E_R$. The value of T_R ranges from a few hundred nanoKelvin for heavy alkalis to a few microKelvin for a light atom such as metastable helium, irradiated on its resonance line $2^3S \leftrightarrow 2^3P$.

Subrecoil cooling of free particles. It is possible to circumvent the recoil limit and to reach temperatures T lower than T_R. The basic idea is to create a situation where the photon absorption rate Γ', which is also the jump rate R of the atomic random walk in velocity space, depends on the atomic velocity $v = p/M$ and vanishes for $v = 0$ (Figure 12). For an atom with zero velocity, the absorption of light is quenched. Consequently, there is no spontaneous re-emission and no associated random recoil. One protects in this way ultra-slow atoms (with $v \simeq 0$) from the "bad" effects of the light. On the contrary, atoms with $v \neq 0$ can absorb and re-emit light. In such absorption-spontaneous emission cycles, their velocities change in a random way and the corresponding random walk in $v-$space can transfer atoms from the $v \neq 0$ absorbing states into the $v \simeq 0$ dark states where they remain trapped and accumulate.

Up to now, two sub-recoil cooling schemes have been proposed and demonstrated. In the first one, called *Velocity Selective Coherent Population Trapping* (VSCPT), and investigated by the Paris group in 1988, the vanishing of $R(v)$ for $v = 0$ is achieved by using quantum interference between different absorption amplitudes which becomes fully destructive when the velocity of the atom vanishes. The second one, called Raman cooling, and investigated by the Stanford group in 1992, uses appropriate sequences of stimulated Raman and optical pumping pulses for tailoring the desired shape of $R(v)$. Using these two schemes, it has been possible to cool atoms down to a few nanokelvins.

Sideband cooling of trapped ions. The states $v \simeq 0$ of Figure 12 are sometimes called "dark states" because an atom in these states does not absorb light. Dark-state cooling also exists for ions and is called *sideband cooling* (see Figure 13). Consider an ion trapped in a parabolic potential well. The vibrational motion of the center of mass of this

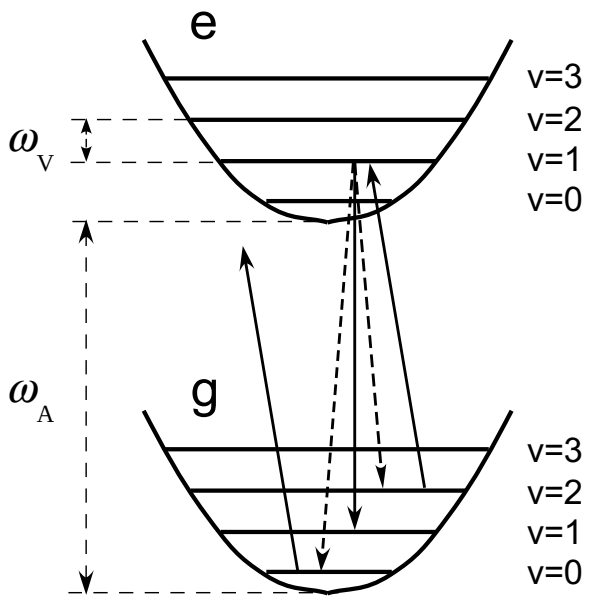

FIGURE 13: Sideband cooling. A laser excitation at frequency $\omega_A - \omega_V$ excites selectively transitions $g, v \longrightarrow e, v-1$, where v is the vibrational quantum number, if the natural width Γ of the excited state is small compared to the vibration frequency ω_V. The most intense spontaneous transitions bringing back the ion to the ground state obey the selection rule $\Delta v = 0$, so that v decreases after such a cycle. When the ion reaches the ground state $g, 0$, it remains trapped here because there are no transitions at frequency $\omega_A - \omega_V$ which can be excited from this state

ion is quantized. The corresponding levels are labelled by a vibrational quantum number $v = 0, 1, 2, ...$ and the splitting between two adjacent levels is equal to $\hbar\omega_V$, where ω_V is the vibrational frequency of the ion in the parabolic potential well. The motion of the center of mass is due to the external electric and magnetic forces acting on the charge of the ion and is, to a very good approximation, fully decoupled from the internal motion of the electrons. It follows that the parabolic potential well and the vibrational levels are the same in the ground electronic state g and in the electronic excited state e (Figure 13). The absorption spectrum of the ion therefore consists of a set of discrete frequencies $\omega_A \pm n\omega_V$, where ω_A is the frequency of the electronic transition, and where $n = 0, \pm 1, \pm 2, ...$ We have a central component at frequency ω_A and a series of "sidebands" at frequencies $\omega_A \pm \omega_V, \omega_A \pm 2\omega_V, ...$ We suppose here that these lines are well resolved, *i.e.* that the natural width Γ of the excited state, which is also the width of the absorption lines, is small compared to their frequency spacing $\omega_V : \Gamma \ll \omega_V$.

The principle of sideband cooling is to excite the ion with laser light tuned at the lower sideband frequency $\omega_A - \omega_V$. One excites in this way the transitions $g, v \longrightarrow e, v-1$. For example, Figure 13 shows the excitation of the transition $g, 2 \longrightarrow e, 1$. After such an excitation in $e, v-1$, the ion falls down in the ground state by spontaneous emission of a photon. One can show that the most probable transition obeys the selection rule

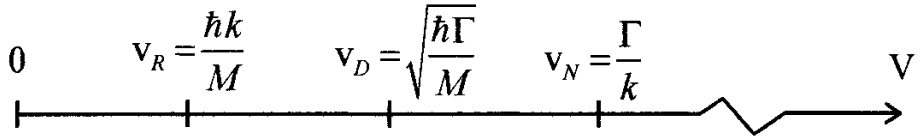

FIGURE 14: A few characteristic velocities associated with the various cooling schemes.

$\Delta v = 0$. For the example of Figure 13, the ion falls preferentially in $g, 1$. There are also much weaker transitions corresponding to $\Delta v = \pm 1$, the ion falling in $g, 0$ and $g, 2$. It is thus clear that the cycle consisting of the excitation by a lower sideband followed by a spontaneous emission process decreases the vibrational quantum number v. After a few such cycles the ion reaches the vibrational ground state $g, v = 0$. It is then trapped in this state because there is no possible resonant excitation from $g, 0$ with a laser light with frequency $\omega_{\rm A} - \omega_{\rm V}$. The transition with the lowest frequency from $g, 0$ is the transition $g, 0 \longrightarrow e, 0$ with frequency $\omega_{\rm A}$ (see Figure 13). The state $g, 0$ is therefore a dark state and, after a few cycles, the ion is put in this state. Sideband cooling is a very convenient way for preparing a single ion in the vibrational ground state. Strictly speaking, the population of the first vibrational excited state is not exactly equal to zero, because of the non resonant excitation of the transitions $\Delta v = 0$ by the laser light at frequency $\omega_{\rm A} - \omega_{\rm V}$. But if Γ is small enough compared to $\omega_{\rm V}$, this population is negligible.

Velocity scales for laser cooling. To conclude this section, we give in Figure 14 a few characteristic velocities given by the previous analysis and appearing in the velocity scale. The first one, $v_R = \hbar k/M$, is the recoil velocity. The second one, $v_D = \sqrt{\hbar\Gamma/M}$, is such that $Mv_D^2 = \hbar\Gamma$ and thus gives the velocity dispersion which can be achieved by Doppler cooling. The last one, $v_N = \Gamma/k$, satisfies $kv_N = \Gamma$, which means that the Doppler effect associated with v_N is equal to the natural width Γ. It gives therefore the velocity spread of the atoms which can be efficiently excited by a monochromatic light. It is easy to check that v_N/v_D and v_D/v_R are both equal to $\sqrt{\hbar\Gamma/E_R}$ where $E_R = \hbar^2 k^2/2M$ is the recoil energy. For most allowed transitions, we have $\hbar\Gamma \gg E_R$, so that $v_R \ll v_D \ll v_N$ (the v-scale in Figure 14 is not linear). This shows the advantage of laser cooling. Laser spectroscopy with a monochromatic laser beam gives lines whose width expressed in velocity units cannot be smaller than v_N. Doppler cooling reduces the velocity dispersion of the atoms to a much lower value, which however cannot be smaller than v_D. Sisyphus cooling reduces this lower limit to a few v_R. Finally, sub-recoil cooling allows one to go below v_R.

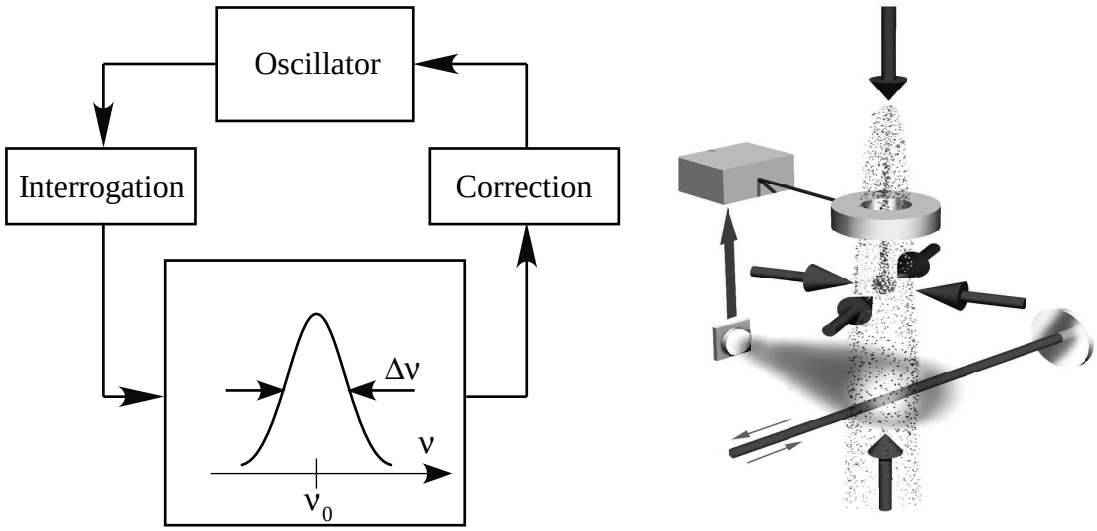

FIGURE 15: Atom clocks. Left: Principle of an atom clock. Right: an atomic fountain

5 Applications of ultra-cold atoms

Ultracold atoms move with very small velocities. This opens new possibilities for basic research and applications. Firstly, ultra-cold atoms can be kept a much longer time in the observation zone than thermal atoms which leave this zone very rapidly because of their high speed. This lengthening of the observation time considerably increases the precision of the measurements. Fundamental theories can be tested with a higher accuracy. Better atom clocks can be built. Secondly, we know since the work of Louis de Broglie that a wave is associated with each material particle, the so-called de Broglie wave. The wave-particle duality, established initially for light, applies also to matter. The wavelength $\lambda_{\rm dB}$ of this wave, called the *de Broglie wavelength* is given, in the non relativistic limit, by the formula $\lambda_{\rm dB} = h/(Mv)$ where h is the Planck constant, M the mass of the particle and v its velocity. Very small values of v thus correspond to large values of $\lambda_{\rm dB}$, which means that the wave aspects of atoms will be easier to observe with ultra-cold atoms than with thermal atoms. We now illustrate these general considerations by a few examples.

5.1 Atom clocks

The principle of an atom clock is sketched in Figure 15 (left). An oscillator (usually a quartz oscillator) is driving a microwave source and its frequency is scanned through an atomic resonance line. This resonance line is centered at the frequency ν_0 of a transition connecting two sublevels a and b of the ground state of an atom and has a width $\Delta\nu$. A servo loop maintains the frequency of the oscillator at the center of the atomic line. In this way, the frequency of the oscillator is locked at a value determined by an atomic frequency

and is the same for all observers. Most atom clocks use cesium atoms. The transition connecting the two hyperfine sublevels a and b of the ground state of this atom is used to define the unit of time: the second. By convention, the second corresponds to 9 192 631 770 periods of oscillations ν_0^{-1}. In usual atom clocks, atoms from a thermal cesium beam pass through two microwave cavities feeded by the same oscillator. The average velocity of the atoms is several hundred m/s; the distance between the two cavities is on the order of 1 m. The microwave resonance line exhibits *Ramsey interference fringes*. The width $\Delta\nu$ of the central component of the signal varies as $1/T$, where T is the time of flight of the atoms from one cavity to another: the larger T, the narrower the central line. For the longest devices, T can reach 10 ms, leading to values of $\Delta\nu$ on the order of 100 Hz.

Much narrower Ramsey fringes, with sub-Hertz linewidths can be obtained in the so-called Zacharias *atomic fountain* (see Figure 15, right). Atoms are captured in a magneto-optical trap and laser cooled before being launched upwards by a laser pulse through a microwave cavity. Because of gravity they are decelerated, they return and fall back, passing a second time through the cavity. Atoms therefore experience two coherent microwave pulses, when they pass through the cavity, the first time on their way up, the second time on their way down. The time interval between the two pulses can now be on the order of 1 second, *i.e.* about two orders of magnitude longer than with usual clocks. Atomic fountains have been realized for sodium in the group of Steven Chu in Stanford and cesium in the group of André Clairon and Christophe Salomon in Paris. A short-term relative frequency stability of $4 \times 10^{-14}\tau^{-1/2}$, where τ is the integration time, has been recently measured for a one meter high Cesium fountain . This stability reaches now the fundamental quantum noise induced by the measurement process: it varies as $N^{-1/2}$, where N is the number of detected atoms. The long term stability of 6×10^{-16} is most likely limited by the hydrogen maser which is used as a reference source. The real fountain stability, which will be more precisely determined by beating the signals of two fountain clocks, is expected to reach $\Delta\nu/\nu \sim 10^{-16}$ for a one day integration time. In addition to the stability, another very important property of a frequency standard is its accuracy. Because of the very low velocities in a fountain device, many systematic shifts are strongly reduced and can be evaluated with great precision.With an accuracy of 2×10^{-15}, the Paris fountain is presently the most accurate primary standard. A factor 10 improvement in this accuracy is expected in the near future. In addition cold atom clocks designed for a reduced gravity environment are currently being built and tested, in order to increase the observation time beyond one second. These clocks should operate in space in relatively near future.

Atom clocks working with ultra-cold atoms can of course provide an improvement of the Global Positioning System (GPS). They could also be used for basic studies. A first line of research consists in building two fountains clocks, one with cesium and one with rubidium atoms, in order to measure with a high accuracy the ratio between the hyperfine frequencies of these two atoms. Because of relativistic corrections, the hyperfine frequency is a function of $Z\alpha$, where α is the fine structure constant and Z is the atomic number. Since Z is not the same for cesium and rubidium, the ratio of the two hyperfine frequencies

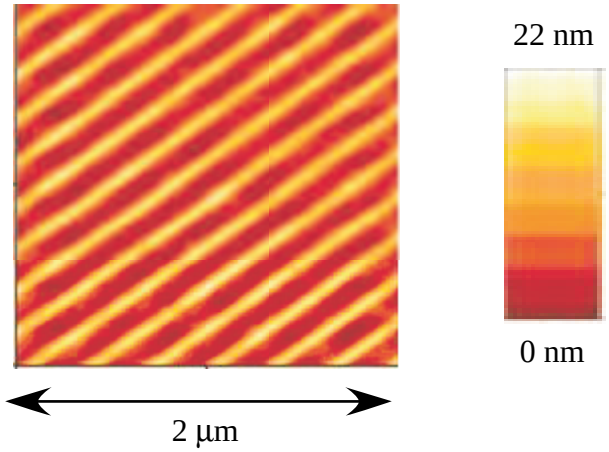

FIGURE 16: Atomic force microscopy image of lines of chromium atoms channeled by a laser standing wave and deposited on a silicon substrate. The width of the lines is 63 nm and the period is 213 nm (Photograph: courtesy of T. Pfau and J. Mlynek).

depends on α. By making several measurements of this ratio over long periods of time, one could check cosmological models predicting a variation of α with time. The present upper limit for $\dot{\alpha}/\alpha$ in laboratory tests could be improved by two orders of magnitude. Another interesting test would be to measure with a higher accuracy the gravitational red shift and the gravitational delay of an electromagnetic wave passing near a large mass (Shapiro effect).

5.2 Atom optics and interferometry

Atom lithography. The possibility to control the transverse degrees of freedom of an atomic beam with laser light opens interesting perspectives in the domain of lithography. One uses the resonant dipole force created by a laser to guide the atoms of a beam and deposit them onto a substrate, where they form the desired pattern. Using for example a standing laser wave orthogonal to the beam axis to channel the atoms at the nodes or antinodes of the wave (depending on the sign of the detuning Δ, see § 3.3), several groups have succeeded in depositing regular atomic patterns (see Figure 16). The typical length scale of these patterns is a few tens of nanometers, which makes this technique competitive with other processes of nanolithography. Efforts are currently being made to adapt this technique to atoms of technological interest (indium, gallium).

Young slit interferometer. Because of the large value which can be achieved for atomic de Broglie wavelengths, a new field of research, atom interferometry, has experienced during the last few years a considerable development. It consists in extending to atomic de Broglie waves the various experiments which were previously achieved with

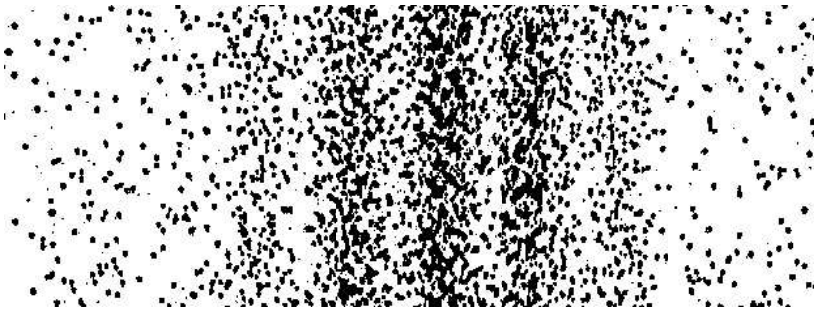

FIGURE 17: Young fringes observed with metastable Neon atoms (photograph: courtesy of F. Shimizu).

electromagnetic waves. For example, Young fringes have been observed in the Laboratory of Fujio Shimizu in Tokyo by releasing a cloud of cold atoms in a metastable state above a screen pierced with two slits. The impact of the atoms on a detection plate is then observed giving a clear evidence of the wave-particle duality. Each atom gives rise to a localized impact on the detection plate. This is the particle aspect. But, at the same time, the spatial distribution of the impacts is not uniform (see Figure 17). It exhibits dark and bright fringes which are nothing but the Young fringes of the de Broglie waves associated with the atoms. Each atom is therefore at the same time a particle and a wave, the wave aspect allowing one to get the probability to observe the particle at a given place.

Ramsey-Bordé interferometers. The existence of internal atomic levels brings an important degree of freedom for the design and the application of atom interferometers. The general scheme of an interferometer using this degree of freedom is represented in fig. 18. The atoms are modelled by a two level system, g being the ground state and e an excited state. They interact with two pairs of laser beams, perpendicular to the atomic beam and separated in space. We suppose that spontaneous emission processes are negligible during the whole interaction time. An atom initially in g with a momentum $p_z = 0$ in the direction z of the laser beams emerges from the first interaction zone in a coherent linear superposition of $g, p_z = 0$ and $e, p_z = \hbar k$ because of the transfer of linear momentum in the absorption process. This explains the appearance of two distinct trajectories differing by both the internal and external quantum numbers in the region between the two lasers of the first pair. After the second interaction zone, there is a certain amplitude that the state $e, p_z = \hbar k$ is transformed into $g, p_z = 0$ by a stimulated emission process while the state $g, p_z = 0$ remains unaffected (left of fig. 18). Another possibility is that the state $e, p_z = \hbar k$ remains unaffected while the state $g, p_z = 0$ is transformed into $e, p_z = \hbar k$ (right of fig. 18). Finally, the interaction with the second pair of laser beams propagating in the opposite direction can close the two paths of each interferometer. Two relevant interference diagrams therefore occur in such a scheme. In the first one (left of fig. 18), the atoms are in the ground state in the central zone between

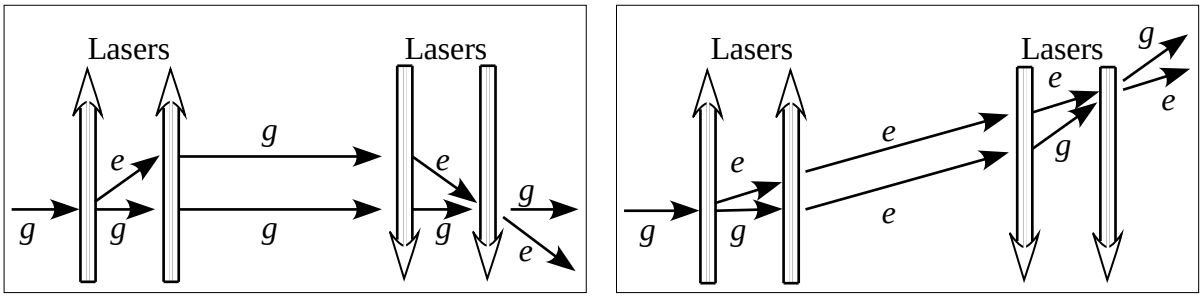

FIGURE 18: The two interferometers arising in the Ramsey-Bordé type geometry. Two-level atoms interact with two pairs of laser waves which induce a coherent coupling between the two internal levels g and e. The horizontal axis may represent time as well as space. The vertical axis is used to represent the recoil of an atom after the absorption or the stimulated emission of a photon. Depending on the experimental conditions, this interferometer can be used to measure rotations perpendicular to the plane of the figure or accelerations. If one adjusts the frequency of the lasers to maximize the interference signal, it constitutes the prototype of an optical clock.

the two pairs of beams. In the second interferometer (right), the atoms are in the excited state in the central zone. Note that the four interactions are separated here in space. The scheme can be easily transposed to a situation where these four interactions are separated in time, the atom being initially in g at rest.

Depending on the geometry of the experiment, the two interferometers of Fig. 18 are sensitive to the frequency of the exciting lasers (thus forming an atomic clock in the optical domain), to the acceleration of the system or to its rotation (gyroscope). In all cases, cold atoms have brought an important gain of sensitivity, thanks to their small velocity. Consider for example the case of the detection of a rotation around an axis perpendicular to the plane of the interferometer. The measurement is based on the Sagnac effect: the rotation modifies the length difference between the two interfering paths of fig. 18. The best demonstrated sensitivity of atom interferometers to rotation is 6×10^{-10} rad/s for an integration time $T = 1$ s, and the sensitivity improves as $\sqrt{T}$. This result, obtained in the group of Mark Kasevich, is comparable to the best optical gyroscopes. One can show that the sensitivity of these atom gyroscopes is higher than the sensitivity of laser gyroscopes with the same area between the two arms of the interferometer by a factor which can be as large as $mc^2/h\nu$, where m is the mass of the atom and ν the frequency of the photon, a factor which can reach values of the order of 10^{11}!

These atom interferometers can also be used to measure accurately fundamental constants. For example, the measurement of the interference pattern as a function of the frequency of the lasers reveals two different resonances for the two interferometers shown in fig. 18. The frequency difference between the two resonances is related to the recoil shift $\hbar k^2/m$, where k is the wave vector of the light and m the mass of the atom. The measurement of this recoil shift, performed in the group of Steve Chu, can be combined with the measurement of the Rydberg constant and the ratio between the proton and the electron masses $m_{\rm p}/m_{\rm e}$. It then yields a value of the fine structure constant α with a

relative accuracy of 10^{-8}. The precision of this method, whose advantage is that it does not depend on Quantum Electrodynamics calculations, is comparable with the other most accurate methods.

Concluding remarks

The manipulation of atomic particles by electromagnetic fields has led to spectacular new results in the last two decades. The combination of the trapping and cooling methods described in this article allows the temperature of atomic gases to be decreased by several orders of magnitude and to reach the sub-microkelvin region. Conversely the thermal wavelength λ_T of the particles is increased by 4 orders of magnitude with respect to its room temperature value. It reaches values of the order of an optical wavelength when the atoms are cooled at the recoil temperature.

For these low temperatures and large wavelengths, the quantum features of the motion of the atomic center of mass become essential. For example an assembly of cold atoms placed in an optical lattice is a model system for the study of quantum transport in a periodic potential. This allows one to draw profound and useful analogies with condensed matter physics, where one deals with the motion of electrons or holes in the periodic potential existing in a crystal. Another field of application of these large wavelengths is atom interferometry, which is now becoming a common tool for realizing ultra-sensitive sensors of acceleration or rotation.

Systems of cold atoms have played a important role in the development of theoretical approaches to quantum dissipation, based either on a master equation for the density operator of the system, or on a stochastic evolution of its state vector. The study of sub-recoil laser cooling has also brought some interesting connections with modern statistical physics problems, by pointing out the possible emergence of Levy flights in the dynamics of these atoms.

When the spatial density ρ of the laser cooled atoms increases, collective processes occur. The formation of molecules assisted by light, or *photoassociation*, has been a very fruitful theme of research where new information could be collected from these ultra-cold molecular systems. Conversely this formation of molecules in laser cooled atomic gases limits the achievable spatial density. This has so far prevented one from reaching the threshold for quantum degeneracy ($\rho\lambda^3 \geq 1$) with purely optical cooling: Bose-Einstein condensation of a bosonic atom gas is observed only when a final step of evaporative cooling is used, after an initial pre-cooling provided by the optical methods described above (see the contribution of Chris Foot and William Phillips in this book).

To summarize, the manipulation of atoms with light is nowadays a tool that is encountered in most atomic physics laboratories. It plays a central role in modern metrology devices, and they are at the heart of the new generation of atom clocks. It is also an essential element for the practical implementation of quantum information concepts (see

the contribution of *** in this book). Thanks to the development of miniaturized systems, cold atoms can be used in very diverse environments, on Earth or even in space: The time provided by a cold atom clock will soon be available from the International Space Station!

References

[1] A more detailed presentation can be found with the text of the three Nobel lectures of 1997: S. Chu, Rev. Mod. Phys. **70**, 685 (1998), C. Cohen-Tannoudji, Rev. Mod. Phys. **70**, 707 (1998), and W.D. Phillips, Rev. Mod. Phys. **70**, 721 (1998).

[2] C.S. Adams and E. Riis, *Laser Cooling and Trapping of Neutral Atoms*, Progress in Quantum Electronics **21**, p. 1-79 (1997).

[3] E. Arimondo, W.D. Phillips, and F. Strumia (editors), *Laser Manipulation of Atoms and Ions*, Proceedings of the 1991 Varenna Summer School (North Holland, Amsterdam, 1992).

[4] H. Metcalf and P. van der Straten, *Laser Cooling and Trapping*, Series: Graduate Texts in Contemporary Physics (Springer 1999).

[5] C. Cohen-Tannoudji, J. Dupont-Roc and G. Grynberg, *Atom-photon interactions – Basic processes and applications*, (Wiley, New York, 1992).

[6] M.O. Scully and M.S. Zubairy, *Quantum Optics*, (Cambridge University Press, 1997).